



1 **Revising the definition of anthropogenic heat flux from** 2 **buildings: role of human activities and building storage heat** 3 **flux**

4 Yiqing Liu¹, Zhiwen Luo¹, Sue Grimmond²

5 ¹ School of the Built Environment, University of Reading, Reading, UK

6 ² Department of Meteorology, University of Reading, Reading, UK

7 *Correspondence to:* * Zhiwen Luo (z.luo@reading.ac.uk) and Sue Grimmond (c.s.grimmond@reading.ac.uk)

8 **Abstract.** Buildings are a major source of anthropogenic heat emissions, impacting energy use and human
9 health in cities. The difference between building energy consumption and building anthropogenic heat emission
10 magnitudes and time lag and are poorly quantified. Energy consumption (Q_{EC}) is a widely used proxy for the
11 anthropogenic heat flux from buildings ($Q_{F,B}$). Here we revisit the latter's definition. If $Q_{F,B}$ is the heat emission
12 to the outdoor environment from human activities within buildings, we can derive it from the changes in energy
13 balance fluxes between occupied and unoccupied buildings. Our derivation shows the difference between Q_{EC}
14 and $Q_{F,B}$ is attributable to a change in the storage heat flux induced by human activities (ΔS_{o-u}) (i.e., $Q_{F,B} =$
15 $Q_{EC} - \Delta S_{o-u}$). Using building energy simulations (EnergyPlus) we calculate the energy balance fluxes for a
16 simplified isolated building (obtaining $Q_{F,B}$, Q_{EC} , ΔS_{o-u}) with different occupancy states. The non-negligible
17 differences in diurnal patterns between $Q_{F,B}$ and Q_{EC} caused by thermal storage (e.g. hourly $Q_{F,B}$ to Q_{EC} ratios
18 vary between -2.72 and 5.13 within a year in Beijing, China). Negative $Q_{F,B}$ can occur as human activities can
19 reduce heat emission from building but are associated with a large storage heat flux. Building operations (e.g.,
20 open windows, use of HVAC system) modify the $Q_{F,B}$ by affecting not only Q_{EC} but also the ΔS_{o-u} diurnal
21 profile. Air temperature and solar radiation are critical meteorological factors explaining day-to-day variability
22 of $Q_{F,B}$. Our new approach could be used to provide data for future parameterisations of both anthropogenic heat
23 flux and storage heat fluxes from buildings. It is evident that storage heat fluxes in cities may also be impacted
24 by occupant behaviour.

25 **1 Introduction**

26 Human's activities that influence energy exchanges are critical to a wide variety of disciplines (e.g.
27 meteorology, building design, geography, climatology, hydrology, engineering). As disciplines often have
28 interests in different scales, purposes and/or boundary conditions, the terminology and acceptable assumptions



29 differ. However, disciplines may provide data to each other or help improve assumptions used. In this study we
30 are concerned with the interface between meteorology, climatology and building design in urban areas.
31 To model the weather and climate in urban areas, an important additional source of energy to the environment is
32 the anthropogenic heat flux (Q_F). This is defined as the heat converted from consumption of biological,
33 chemical and electrical energy and released to the atmosphere due to human activities (Oke et al., 2017). Q_F has
34 three major sources, including metabolic (people and animals) activities ($Q_{F,M}$), transport ($Q_{F,T}$) and buildings
35 ($Q_{F,B}$) (Grimmond, 1992). It can be large relative to incoming solar radiation in summer (e.g. 43% in an area of
36 Beijing (Nie et al., 2014)) and increases air temperature in cities (e.g. (Ichinose et al., 1999; Fan and Sailor,
37 2005)), subsequently contributing to higher cooling demand for buildings (Santamouris et al., 2001; Takane et
38 al., 2019). Apart from that, Q_F is also a dominant attribution of wintertime urban heat island (Biggart et al.,
39 2021). Compared to $Q_{F,M}$ and $Q_{F,T}$, the generated heat within building volume is not all directly ejected into the
40 outdoor environment. For example, the heat from mechanical heating system is released in the indoor
41 environment, then conducted into building fabric and eventually emitted into atmosphere through sensible
42 turbulent heat flux and outgoing longwave radiation. In this process the net storage heat flux (ΔQ_S) of building
43 is modified since building fabric temperature is changed by mechanical heating system with absorbing more
44 heat.

45 In urban areas, ΔQ_S is the net uptake or release of energy from urban volume. This term is an important
46 determinant of urban climate and is regarded as a key process in the genesis of urban heat island (Goward,
47 1981). The change in building ΔQ_S is modified when heat is released by human activities but the timing of the
48 externally emissions are impacted by the building fabric characteristics and the conduction process. With prior
49 studies often using energy consumption (Q_{EC}) as a proxy for $Q_{F,B}$ from inventory related approaches (e.g. Sailor
50 and Lu, 2004; Iamarino et al., 2012) and building energy modelling (e.g. Heiple and Sailor, 2008; Nie et al.,
51 2014), the impact on ΔQ_S is not addressed. To qualify the 'real' $Q_{F,B}$ and change of ΔQ_S , we revisit the
52 definition of $Q_{F,B}$ and attempt to understand how human activities affect the energy balance fluxes of building.

53 If $Q_{F,B}$ is the heat released from buildings into the atmosphere as a result of human activities inside the
54 building (including human metabolism), when the building is completely unoccupied (e.g. no operational
55 appliances, no people) $Q_{F,B}$ is zero. However, heat released from the unoccupied building is non-zero as there is
56 still heat exchange between building and ambient environment. Shortwave and longwave radiation can enter the
57 unoccupied internal building space through windows and conduction through walls. This energy modifies the
58 internal building volume, influencing storage heat flux and the other terms of the energy balance. These are not



59 anthropogenic heat flux when the energy leaves the unoccupied building but influence the heat emissions from
60 the building. This is consistent with radiation penetrating deep into water, and similarly allowing a larger
61 volume to be heated than soil because of convection (Sellers, 1965).

62 For an occupied building, the internal heat gain arises from: (1) the equivalent sources and sinks as the
63 unoccupied buildings; but also (2) the energy linked to the indoor human activities (metabolism, powered
64 appliances and energy inputs to heating or cooling). These will modify each of the energy balance fluxes. Some
65 of this additional energy is transported out of buildings through indoor-outdoor ventilation exchange and
66 immediately contributes to $Q_{F,B}$, while some is stored in the building fabric, and later released outdoors through
67 various pathways (convection, radiation, conduction) to become $Q_{F,B}$ with a time lag. Here, we will derive
68 $Q_{F,B}$ by looking at the difference of heat fluxes between occupied and unoccupied buildings.

69 If the energy balance for the building system (including the indoor air and building envelope) for an
70 unoccupied dry building (assuming latent heat is not important in this case) is:

$$71 \quad Q_{uo}^* = Q_{H,uo} + Q_{BAE,uo} + \Delta Q_{S,uo} \quad (1)$$

72 The radiation balance for an isolated unoccupied (uo) building can be expressed as:

$$73 \quad Q_{uo}^* = K_{\downarrow,uo} - K_{\uparrow,uo} + L_{\downarrow,uo} - L_{\uparrow,uo} \quad (2)$$

74 where Q^* is the net all-wave radiation, K is the shortwave radiation incoming (\downarrow) and outgoing (\uparrow) to the
75 external surfaces. The longwave (L) radiation exchanges depend on the view factors (F) between the building of
76 interest (boi), the surrounding facets of other surfaces/buildings ($other\ b$) and the sky:

$$77 \quad L_{\downarrow,uo} = L_{\downarrow,uo(F[sky \rightarrow boi])} + L_{\downarrow,uo(F[other\ b \rightarrow boi])} \quad (3)$$

$$78 \quad L_{\uparrow,uo} = L_{\uparrow,uo(F[boi \rightarrow sky])} + L_{\uparrow,uo(F[boi \rightarrow other\ b])} \quad (4)$$

79 In Eq. (1), Q_H is the turbulent sensible heat flux (convection) from external surfaces to the external ambient
80 air. Q_{BAE} is the net energy exchange from the buildings through air exchange (e.g. ventilation). When the
81 building is sealed Q_{BAE} is 0 W m^{-2} , otherwise (e.g. open windows, cracks) it can be a source or sink of energy
82 (environment \leftarrow building, or inverse). ΔQ_S is the net storage heat flux of the building volume (i.e. fabric,
83 contents, including the air). The left-hand side (LHS) of Eq. (1) is the inputs or source of energy to the building,
84 whereas the right-hand side (RHS) is the sink or energy dissipation outputs. With no human activities within the
85 building and the internal heat generation from human and infrastructure activities is zero.

86 When the building is occupied (o) (e.g. appliances operating) additional terms are needed in Eq. (1) to
87 account for the supply of energy into the building for these activities and the release of energy:

$$88 \quad Q_o^* + Q_{Internal,o} + Q_{HVAC,o} = Q_{H,o} + Q_{BAE,o} + \Delta Q_{S,o} + Q_{Waste,o} \quad (5)$$



89 The two additional sources of energy (LHS) are:

90 (1) $Q_{Internal,o}$: energy released within the building from lighting, powered appliances and metabolism (e.g.
91 people, pets).

92 (2) $Q_{HVAC,o}$: energy consumption in the building from heating, ventilation and air conditioning (HVAC) system.

93 As the building may emit exhaust/waste heat (e.g. via HVAC systems), there is an additional sink (RHS)
94 referred to here as $Q_{Waste,o}$.

95 To determine the impact of the occupancy (i.e. not just the physical building form) we can consider the
96 difference between Eq. (5) and Eq. (1). If the radiation balance for the occupied case is:

$$97 \quad Q_o^* = K_{l,o} - K_{t,o} + L_{l,o} - L_{t,o} \quad (6)$$

98 We assume that the incoming and outgoing shortwave radiation remains unchanged because the reflectivity,
99 transmissivity and absorptivity do not change by occupancy activities then:

$$100 \quad K_{l,o} = K_{l,uo}; \quad K_{t,o} = K_{t,uo}$$

101 The incoming longwave radiation is dependent on the surroundings which are independent to the building state,
102 so:

$$103 \quad L_{l,o} = L_{l,uo}$$

104 Thus, the difference of radiative fluxes between occupied and unoccupied building ($\Delta L_{t,o-uo}$) is:

$$105 \quad \Delta L_{t,o-uo} = L_{t,o} - L_{t,uo} \quad (7)$$

106 Similarly, the difference of the heat transfer through air exchange is:

$$107 \quad \Delta BAE_{o-uo} = BAE_o - BAE_{uo} \quad (8)$$

108 With the additional terms in Eq. (5) and the air exchanges rates difference from the activities within the
109 buildings, gives:

$$110 \quad \Delta B_{o-uo} = [Q_{Internal,o} + Q_{HVAC,o}] - [Q_{Waste,o} + \Delta BAE_{o-uo}] \quad (9)$$

111 As the change in surface temperature influences the sensible heat fluxes and storage heat fluxes:

$$112 \quad \Delta H_{o-uo} = H_o - H_{uo} \quad (10)$$

$$113 \quad \Delta S_{o-uo} = \Delta Q_{S,o} - \Delta Q_{S,uo} \quad (11)$$

114 By combining the Eq. (1) and Eq. (5), we obtain:

$$115 \quad \Delta B_{o-uo} = \Delta L_{t,o-uo} + \Delta H_{o-uo} + \Delta S_{o-uo} \quad (12)$$

116 where the LHS accounts for the net available energy as result of human activities in indoor environments and
117 the RHS shows that these impact the longwave radiation, turbulent sensible and storage heat fluxes (in this dry
118 case). With rearrangement:



$$119 \quad [Q_{Internal,o} + Q_{HVAC,o}] = \Delta S_{o-uo} + [\Delta L_{\uparrow,o-uo} + \Delta H_{o-uo} + \Delta BAE_{o-uo} + Q_{Waste,o}] \quad (13)$$

120 The additional energy generation associated with human activities to the whole building system (LHS) is
121 apparent, as traditionally defined as $Q_{F,B}$ previously (Heiple and Sailor, 2008). Here because the heat release
122 from human metabolism indoors is considerably smaller than other sources, for simplicity of analysis, we
123 assume metabolic heat is also part of energy consumption ($Q_{EC} = Q_{Internal,o} + Q_{HVAC,o}$). Besides, some of
124 additional energy is associated with the extra gain or release of stored heat within the building volume (ΔS_{o-uo}).
125 The rest is the heat released to outdoor environment from building due to human activities, which is the $Q_{F,B}$
126 based on its definition:

$$127 \quad Q_{F,B} = \Delta L_{\uparrow,o-uo} + \Delta H_{o-uo} + \Delta BAE_{o-uo} + Q_{Waste,o} \quad (14)$$

128 Eq. (14) demonstrates the $Q_{F,B}$ is the relative heat emission at exterior building boundary between
129 unoccupied and occupied building through longwave radiation, convection, air exchange and waste heat from
130 mechanical heating/cooling system. The source of $Q_{F,B}$ within the building volume gives (by combining Eq.
131 (13) and Eq. (14):

$$132 \quad Q_{F,B} = Q_{EC} - \Delta S_{o-uo} \quad (15)$$

133 The sources of $Q_{F,B}$ are from both energy consumption (Q_{EC}) and difference of storage heat flux (ΔS_{o-uo})
134 between unoccupied and occupied building ($Q_{F,B}$ in this study includes part of $Q_{F,M}$ from human metabolism).
135 Whereas the second term is ignored in most prior studies and consequently leads to a time lag and magnitude
136 difference between $Q_{F,B}$ and Q_{EC} (Sailor, 2011). Therefore, estimation of $Q_{F,B}$ by differences in heat emission
137 between occupied and unoccupied building can capture impact of dynamic changes in the building storage heat
138 flux.

139 In this study, the objective is to understand the temporal profile of $Q_{F,B}$, and how and why it differs from
140 Q_{EC} at diurnal and seasonal time scales, by examining differences in energy balance fluxes between an occupied
141 and unoccupied same building. Building energy simulation tool (EnergyPlus) is used to obtain the various
142 energy balance fluxes from the building system.

143 2 Methods

144 2.1 Unoccupied (uo) and occupied (o) building energy simulation (BES)

145 Building energy simulation (BES) is widely used to estimate energy consumption, heat emission and heat
146 storage within a building, while allowing changes in heat fluxes due to human activities to be estimated. Here



147 we use EnergyPlus version 9.4 (DOE, 2020) to study an isolated building (i.e. without a surrounding
148 neighbourhood). The ASNI/ASHRAE standard 140 Case 900 test model (ASHRAE, 2017) is used, which is
149 developed in a software-to-software comparative tests for validating building thermal load. It is a 48 m² one-
150 story heavyweight rectangular prism with high mass fabrics (Appendix A), whose simple geometry is ideal to
151 understand the process of how human activities change the building energy balance fluxes in a theoretical study.
152 Modifications of the original building model for this study, include: windows are reduced to one (6 m² south-
153 facing) for more appropriate EnergyPlus single-sided ventilation calculations (Daish et al., 2016); and internal
154 heat gain, ventilation control strategy and HVAC system operation vary with different scenarios considered
155 (Table 1). For the simulations, the building is assumed to be located in Beijing as the climate has both hot
156 summer and cold winter conditions. Chinese Standard Weather Data (CSWD) selected to create a Typical
157 Meteorological Year (TMY) (China Meteorological Bureau et al., 2005) are used as the meteorological forcing,
158 as these data are developed for simulating building thermal load and energy use.

159 The modelling scenarios (Table 1) vary with building occupation state. Two types of unoccupied (*uo*)
160 buildings are considered. Neither have internal heat gains nor HVAC systems, but they differ based on air
161 exchange between (1) unoccupied sealed (*us*) with no infiltration or ventilation, and (2) unoccupied ventilated
162 (*uv*) with 50% of windows area kept open. The single-sided natural ventilation rate is estimated by including
163 both wind-driven ventilation rate (V_W , m³ s⁻¹) (Warren 1977):

$$164 \quad V_W = 0.025A_{eff}U_W \quad (16)$$

165 and the stack buoyancy-driven ventilation rate (V , m³ s⁻¹) (Warren 1977):

$$166 \quad V_{Stack} = \frac{1}{3}A_{eff}C_d\sqrt{\frac{\Delta THg}{T_{ave}}} \quad (17)$$

167 where A_{eff} is the effective opening area (m²), U_W is reference wind speed at the height of opening (m s⁻¹). C_d
168 is discharge coefficient (usually taken as 0.6 (Wang and Chen, 2012)), ΔT is indoor and outdoor air temperature
169 difference (°C), H is the height of opening (m), g the gravitational acceleration (m s⁻²), T_{ave} is average indoor
170 and outdoor air temperature (°C). The combined ventilation rate is (Fan et al., 2021):

$$171 \quad V_T = \sqrt{V_W^2 + V_{Stack}^2} \quad (18)$$

172 The three occupied (*o*) building simulations assume occupant behaviour modifies internal heat generation,
173 natural ventilation and HVAC systems (*ov*). First, *ov1* has internal heat gains ($Q_{Internal,o}$) from human
174 metabolism, lighting and other appliances based on local building code (MOHURD, 2018), with window always



175 open (50%, as uv). The internal heat gains are held constant allowing the fraction of heat in $Q_{F,B}$ and ΔQ_S to be
 176 impacted by building and climate conditions but not the diurnal variability of human heat generation.

177 Second, $ov2$ considers natural ventilation based on passive cooling and thermal comfort. The window
 178 opening is controlled automatically. It is opened (50% of window area) when the indoor air temperature is
 179 higher than both outdoor air temperature and ventilation setpoint (23°C for ‘warm limit’ in bedroom
 180 (Oikonomou et al., 2012)). Otherwise, it is closed to reduce heat loss and keep the building warm. Third, since
 181 natural ventilation alone may not satisfy indoor thermal comfort, mixed mode ventilation with auxiliary HVAC
 182 system (e.g. Wang and Chen, 2013; Wang and Greenberg, 2015; Chen et al., 2017) is considered in $ov3$. The
 183 mechanical heating and cooling system are active when indoor temperature reaches the threshold (18°C for
 184 heating and 26°C for cooling, MOHURD, 2018). The ventilation control strategy in $ov3$ is the same as $ov2$, but
 185 the EnergyPlus hybrid ventilation manager (DOE, 2020) turns the HVAC off when natural ventilation is active
 186 to prevent simultaneous operation.

187 Table 1. Cases simulated differ based on building occupation state, internal heat gain ($Q_{Internal,o}$) and presence of natural
 188 ventilation and HVAC. Notation are defined in text and nomenclature

Code	Occupation state	Natural ventilation	$Q_{Internal,o}$ (W m ⁻²)	Window open Temperature control (°C)	HVAC Heating/cooling setpoint (°C)
us	uo	Sealed	0	N/A	N/A
uv	uo	Window always open (50%)	0	N/A	N/A
ov1	o	Window always open (50%)	11.8	N/A	N/A
ov2	o	Controlled ventilation	11.8	23	N/A
ov3	o	Mixed mode control	11.8	23	18/26

189 2.2 Determination of anthropogenic heat flux

190 The simulated hourly heat fluxes by radiation, convection, air exchange and waste heat generated from HVAC
 191 system between the isolated building and atmosphere (Table A.3) are analysed for each case (Table 2). If
 192 cooling occurs, the waste heat consists of the cooling load and electrical energy consumed by the air conditioner
 193 (Q_{HVAC}). Q_{HVAC} is predicted using a static coefficient of performance (COP) for the air conditioner, and the heat
 194 removed by an air conditioner (Q_{AC}) to the total amount of electricity consumed:

$$195 \quad Q_{HVAC,c} = \frac{Q_{AC}}{COP} \quad (19)$$

$$196 \quad Q_{Waste,c} = Q_{AC}(1 + COP^{-1}) \quad (20)$$

197 With a centralised heating system (as Beijing has), for simplicity we assume all energy associated with the
 198 heating system is released indoors, and waste heat due to boiler efficiency and pipe heat loss are not considered:

$$199 \quad Q_{HVAC,H} = Q_{HS} \quad (21)$$



200 $Q_{Waste,H} = 0$ (22)

201 Combining these, and accumulated though time gives annual values:

202 $Q_{HVAC} = Q_{HVAC,C} + Q_{HVAC,H} = \frac{Q_{AC}}{COP} + Q_{HS}$ (23)

203 $Q_{Waste} = Q_{Waste,C} + Q_{Waste,H} = Q_{AC}(1 + COP^{-1})$ (24)

204 Each term in Eq. (14) is determined using an occupied (*o*) and unoccupied (*uo*) building result to determine
205 $Q_{F,B}$ and the other fluxes. The results are analysed by season (spring (March, April and May; MAM), summer
206 (JJA), autumn (SON) and winter (DJF)) using the median (50%) and interquartile range (IQR) between the 25th
207 and 75th percentiles to assess the diurnal patterns.

208 2.3 Ratio of anthropogenic heat flux to energy consumption

209 If the energy consumed within the building is rejected immediately into the atmosphere (Heiple and Sailor,
210 2008), the change in ΔQ_S is not accounted for, and therefore $Q_{F,B}$ is assumed to be only from energy
211 consumption (Q_{EC}). The variation of ΔQ_S associated with human activities is considered when using the relative
212 heat emissions in Eq. (14) and Eq. (15). We use the ratio $R = \frac{Q_{F,B}}{Q_{EC}}$ to determine the relative importance of
213 building operation modes and choice of baselines on the discrepancy between $Q_{F,B}$ and Q_{EC} .

214 3 Results and discussion

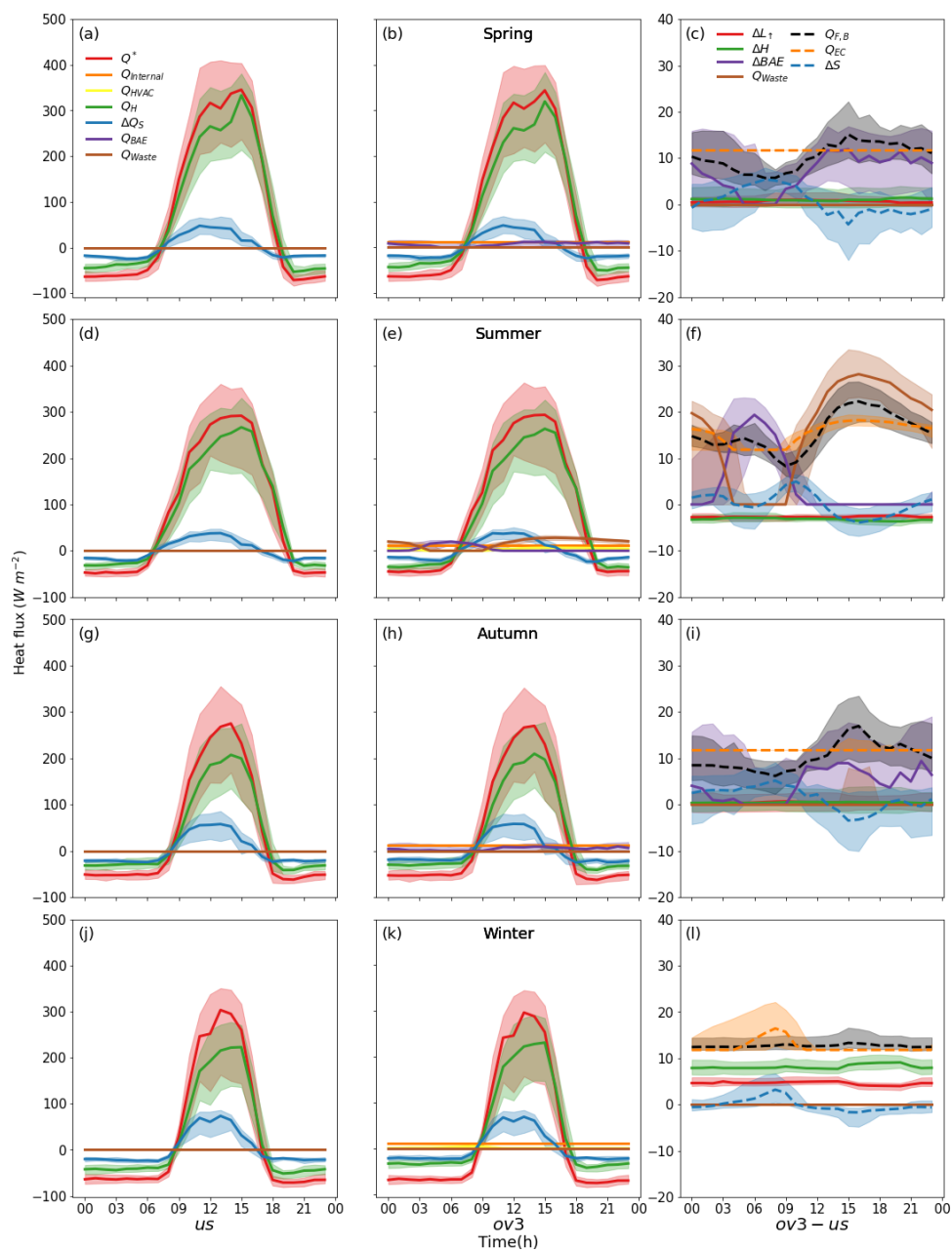
215 Building energy balance fluxes vary through each day and season (Fig. 1) associated with when a building is
216 occupied and people's activities inside the building. First, we consider one case in detail - an occupied building
217 with both natural ventilation and HVAC (*ov3*, Table 3) relative to an unoccupied sealed building (*us*, Table 4) -
218 their difference (*ov3-us*) allows us to obtain the fluxes needed (Sect. 1).

219 As noted (Sect. 1), the shortwave and incoming longwave radiative fluxes for all cases (Table 5) are
220 assumed identical, but all other terms of the building energy balance differ. Hence, the change in outgoing
221 longwave radiation ($\Delta L_{\uparrow,o-uo}$, Fig. 1c) is equivalent to the net all-wave radiation difference (Q_{o-uo}^* , Fig. 1a-b)
222 for the occupied and unoccupied buildings. The positive sensible heat flux difference (Eq. (10), ΔH_{o-uo} , Fig. 1c)
223 and $\Delta L_{\uparrow,o-uo}$ indicate the building is warmed up by internal heat gains ($Q_{Internal,o}$) with higher exterior surface
224 temperatures. Their small magnitudes and flat patterns indicate small relative importance compared to the heat
225 exchange from ventilation differences (Eq. (8), ΔBAE_{o-uo} , Fig. 1c). The latter, not only contributes the largest
226 fraction of anthropogenic heat flux ($Q_{F,B}$, Fig. 1c), but also has a diurnal pattern consistent with $Q_{F,B}$, especially



227 during spring and autumn (Fig. 1c, i). Rarely, heat ($Q_{Waste,o}$, Fig. 1i) is emitted by the air conditioner in the
228 mid-afternoon (shading) at this time of year, but more importantly in summer (Fig. 1f) when cooling demand
229 increases.

230 $Q_{F,B}$ (Eq. (14), Fig. 1c) has four components of emitted heat, whereas energy consumption (Q_{EC} , Fig. 1c)
231 only has (in this case, constant) internal heat gains ($Q_{Internal,o} = 11.8 \text{ W m}^{-2}$, Fig. 1b, Table 6) and energy use
232 from HVAC system (Q_{HVAC} , Fig. 1b). Their difference is the storage heat flux difference (Eq. (15) ΔS_{o-u_0} in Fig.
233 1c). If ΔS_{o-u_0} is positive, the building acts as a heat sink and stores the extra heat generated by human activities,
234 or stored heat is released when ΔS_{o-u_0} is negative. Hence, we can identify the impacts of seasonal-varying
235 human activities and building operations on the diurnal variability in ΔS_{o-u_0} , Q_{EC} and $Q_{F,B}$.



236

237 Figure 1: Seasonal diurnal median (line) and inter-quantile range (IQR, shading) building heat fluxes for (a, d, g, j)
 238 unoccupied sealed (us), (b, e, h, k) occupied ventilated (ov3) building and their (c, f, i, l) difference (ov3-us) for (a-c) spring,
 239 (d-f) summer, (g-i) autumn and (j-l) winter. $Q_{F,B}$ is estimated by either heat transfer difference (solid line components):
 240 $Q_{F,B} = \Delta L_{\tau,0-u0} + \Delta H_{0-u0} + \Delta BAE_{0-u0} + Q_{Waste,0}$ in Eq. (14) or energy consumption and storage flux difference: $Q_{F,B} =$
 241 $Q_{EC} - \Delta S_{0-u0}$ (dash line components) in Eq. (15)



242 3.1 Impact of human activities on seasonal and diurnal variations of the fluxes

243 For the same *ov3-us* case (Table 1, Fig. 1), we consider the temporal and seasonal variability of the fluxes. In
244 spring and autumn (Fig. 1a-c, g-i), natural ventilation is the dominant factor contributing to diurnal variation in
245 ΔS_{o-u_0} and $Q_{F,B}$, while Q_{EC} has minimal variability. Q_{EC} is slightly larger than $Q_{Internal,o}$ because of some
246 short periods of HVAC use in the mid-afternoon (IQR shading in Fig. 1i). There is a clear diurnal cycle of $Q_{F,B}$
247 (Fig. 1c) with the median varying between 8 W m^{-2} (07:00) and 15 W m^{-2} (15:00) relative to the constant
248 internal heat gain (11.8 W m^{-2}). The difference between $Q_{F,B}$ and Q_{EC} (ΔS_{o-u_0}) is largely impacted by natural
249 ventilation. During the night and early morning with closed window, only part of the consumed energy is
250 transferred externally to the atmosphere. The rest of the heat is stored in the building fabric (positive ΔS_{o-u_0}),
251 hence $Q_{F,B}$ is lower than Q_{EC} . However, when overheating may occur during the middle of the day, occupants
252 keep window opened (air conditioner is less frequently used) to cool the building down, with stored heat
253 released (negative ΔS_{o-u_0}). This is consistent with the diurnal variability of ΔBAE_{o-u_0} which has a minimum at
254 night (window closed) and maximum in the mid-noon (window open).

255 In summer, the role of natural ventilation at daytime is replaced by air conditioning. Natural ventilation and
256 waste heat from the air conditioner ($Q_{Waste,o}$) contribute to one peak $Q_{F,B}$ at nighttime and daytime, respectively
257 (Fig. 1f). $Q_{F,B}$ is higher than Q_{EC} around these two peak periods (05:00-07:00 and 13:00-21:00). The peak $Q_{F,B}$
258 at night reaches 14 W m^{-2} (median) at 05:00, which is mainly attributed to natural ventilation when outdoor air
259 temperature is cooler than indoors. Conversely, in the afternoon when outdoor temperature is warmer, occupants
260 ‘choose’ mechanical cooling for achieving thermal comfort. The peak $Q_{F,B}$ is 22 W m^{-2} at 16:00, approximately
261 22% higher than Q_{EC} . It indicates that using Q_{EC} for the anthropogenic heat flux from buildings (e.g. Heiple and
262 Sailor, 2008) may underestimate the effect of $Q_{F,B}$ on urban atmospheric processes especially during the late
263 afternoon/early evening. In addition, $Q_{F,B}$ is always smaller than $Q_{Waste,o}$ because of the negative $\Delta L_{\uparrow,o-u_0}$ and
264 ΔH_{o-u_0} causing a cooler exterior surface. This suggests using $Q_{Waste,o}$ as $Q_{F,B}$ (e.g. Chow et al., 2014) may
265 overestimate $Q_{F,B}$ in summer.

266 However, in winter, mechanical heating and thermal mass effect shape the temporal pattern of $Q_{F,B}$ (Fig.
267 1i). The cool outdoor air temperature before sunrise results in a substantial heating load and peak Q_{EC} (16.43 W
268 m^{-2} for median line) at 08:00. This heat is stored in building fabric (positive ΔS_{o-u_0}) and have a relatively stable
269 release through convection and longwave radiation. Therefore the diurnal profile $Q_{F,B}$ is rather flatter and
270 ΔS_{o-u_0} has a highly consistent temporal pattern to Q_{EC} .



271 Overall, this analysis recognizes the crucial role of ΔS_{o-u_0} in distinguishing $Q_{F,B}$ from Q_{EC} , which is highly
272 dependent on HVAC operation and natural ventilation (i.e., human activity of opening window). These two
273 factors can rapidly increase or decrease $Q_{F,B}$ while convection and longwave radiation cannot. Whereas in
274 winter, the larger IQR (shading) of $Q_{F,B}$ than Q_{EC} indicates more day-to-day variation in $Q_{F,B}$ diurnal profile
275 than Q_{EC} . Estimates of $Q_{F,B}$ using satellite remote sensing found heat storage plays an important role in
276 moderating energy use within buildings (Yu et al., 2021). As the storage heat flux change modifies the diurnal
277 sensible heat flux pattern it modifies the surface temperature increment ($Q_{F,B}$ in remote sensing approach) and
278 hence the apparent energy consumption.

279 The diurnal profiles of ΔS_{o-u_0} are not identical between seasons as people use different actions to achieve
280 thermal comfort in different weather conditions. This suggests the $Q_{F,B}$ and Q_{EC} differences may vary between
281 climates and with cultural practices. In inventory methods the diurnal profiles may be limited (e.g. LUCY (Allen
282 et al., 2011), weekday/weekend by country) and ignore seasonal variations. However, ΔS_{o-u_0} behaviour types
283 classes may benefit from distinguishing diurnal variation for different climates.

284 3.2 Impact of different building operation modes on seasonal and diurnal variations

285 Fig. 2 illustrates the impact of different building operation modes (Table 1: *ov1*, *ov2*, *ov3*; cf. *us*) on the $Q_{F,B}$
286 diurnal profiles. It suggests the different ventilation strategies and HVAC systems do change $Q_{F,B}$ in both
287 temporal pattern and magnitude, but their impacts vary among seasons.

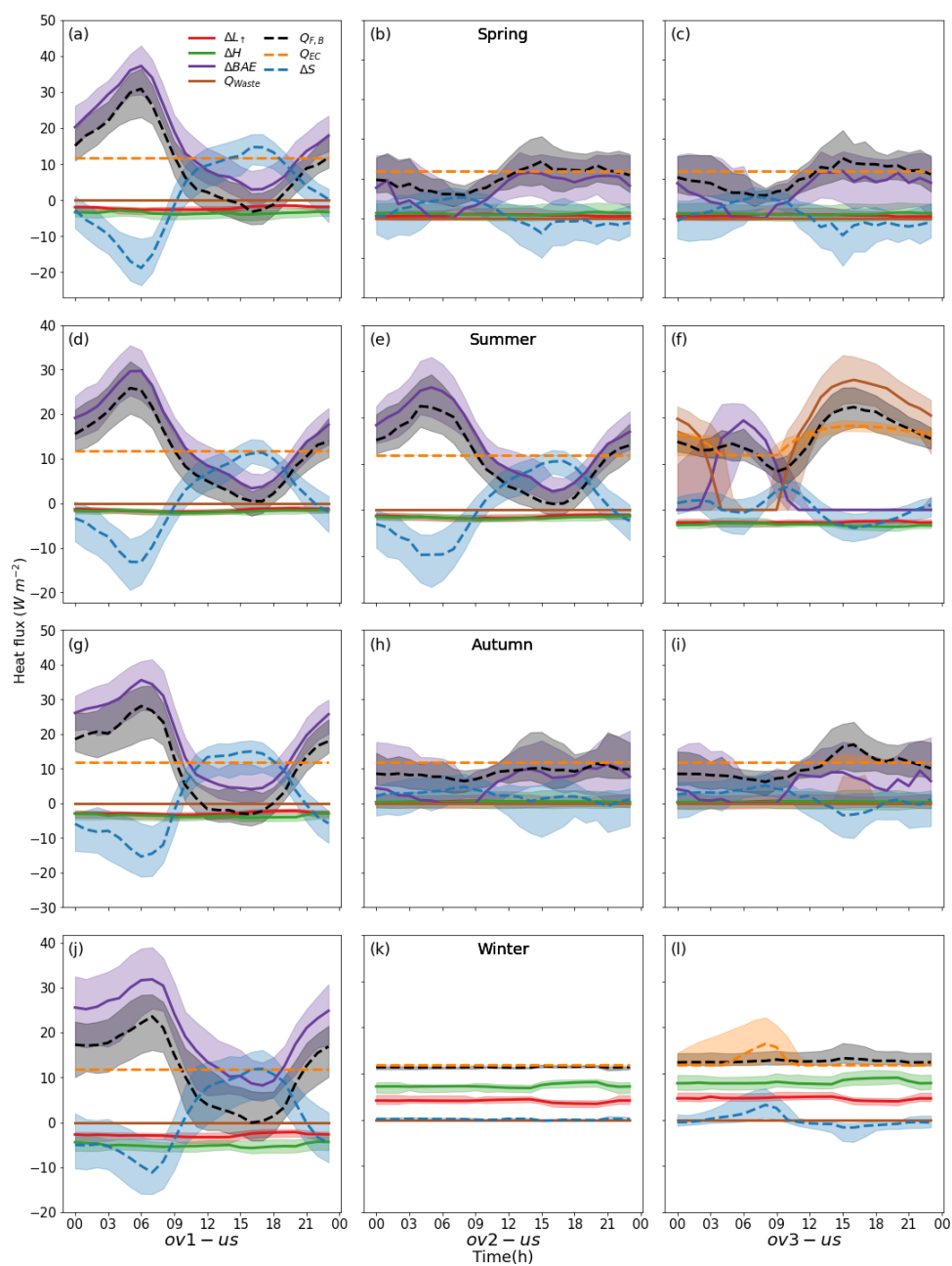
288 In spring and autumn, different natural ventilation control strategies completely modify the $Q_{F,B}$ diurnal
289 profile, whereas HVAC system only increases the peak $Q_{F,B}$ slightly in autumn (Fig. 2i). The distinctly different
290 (opposite) trend in diurnal $Q_{F,B}$ pattern for *ov1* cf. *ov2* or *ov3* (Fig. 2a-c, g-i) is largely explained by the diurnal
291 change of ΔBAE_{o-u_0} in the three cases. In *ov1* (window open, no control) the minimum outdoor air temperature
292 before sunrise creates the maximum indoor and outdoor air temperature difference, therefore the highest
293 ΔBAE_{o-u_0} and peak $Q_{F,B}$ at 06:00 (30 W m⁻² for the median in Fig. 2a). Whereas *ov2* and *ov3* have the window
294 closed at night and early morning to avoid overcooling, therefore the minimum $Q_{F,B}$ in the early morning
295 (07:00). As outdoor air temperature increases through the day, $Q_{F,B}$ follows the reduced ΔBAE_{o-u_0} in *ov1*,
296 whereas natural ventilation is active in *ov2* and *ov3*, leads to an increase in ΔBAE_{o-u_0} and $Q_{F,B}$. Unlike *ov2*, *ov3*
297 has a clear peak (16 W m⁻² median, Fig. 2i) at 15:00, because when natural ventilation alone cannot satisfy
298 thermal comfort and *ov3* air conditioning is activated. But their overall patterns (IQR) are very consistent,
299 indicating afternoon use of air conditioning could increase $Q_{F,B}$ magnitude but have a limited impact on other



300 parts of the diurnal pattern. Surprisingly, negative $Q_{F,B}$ occurs around 17:00 in spring (Fig. 2a), suggesting the
301 occupied building has less heat emissions than unoccupied building. Because the natural ventilation at night and
302 morning cools down the building and reduced fabric exterior surface temperature leads to a large reduction in
303 longwave radiation and convection ($\Delta L_{\tau,o-u0}$ and ΔH_{o-u0}) than increase in heat emission through natural
304 ventilation (ΔBAE_{o-u0}) in afternoon. And the reduced overall emissions are converted into increase in storage
305 heat flux (ΔS_{o-u0}). Negative $Q_{F,B}$ also occurs when unoccupied building is always ventilated (uv) and occupied
306 building is ventilated with control (ov2 and ov3) in spring (e.g. Fig. B6b-c). The window is closed to avoid
307 excessive cooling at night in ov2. With ΔBAE_{o-u0} negative in this case, its magnitude is much larger than
308 increase in longwave radiation and convection ($\Delta L_{\tau,o-u0}$ and ΔH_{o-u0}). The minimum $Q_{F,B}$ frequently
309 corresponds to the peak ΔS_{o-u0} .

310 In summer, ov2 window is open most of the time (as in ov1) for thermal comfort, therefore the $Q_{F,B}$ has no
311 apparent difference to ov1. However for ov3, as air conditioning runs from morning to late night and there is a
312 very different diurnal profile (cf. ov2 and ov1). Air conditioner use contributes to a much larger $Q_{F,B}$ (cf. ov2)
313 from 12:00 to 21:00. Not only is extra energy consumed, but it also removes heat from building to the
314 atmosphere in this period. In contrast, using natural ventilation as a cooling strategy (ov1 and ov2) contributes to
315 a high $Q_{F,B}$ at night and early morning but very low even negative extra heat emission in afternoon.

316 Consistent with results in the other seasons, different ventilation control strategies in winter cause a large
317 change in $Q_{F,B}$ profile between ov1 and ov2. However, the temporal pattern of $Q_{F,B}$ (IQR) in ov2 is quite similar
318 to ov3 because the supplied heat from mechanical heating system does not immediately enhance $Q_{F,B}$ with
319 closed window. ov2 is the only scenario that has similar $Q_{F,B}$ and Q_{EC} through the whole day. Comparison using
320 an unoccupied ventilated (uv) baseline (Fig. B.6) (cf. us Fig. 2) show that although $Q_{F,B}$ profiles differ, the
321 impacts of different building operation modes are consistent when the same occupied buildings used. The
322 impact of baselines with different air exchange on $Q_{F,B}$ are analysed in Sect. 3.3.



323

324 Figure 2 : As Figure 1c, f, i, j , but comparing three different building operation types (a, d, g, j) *ov1*: window is always open

325 without control, no HVAC; (b, e, h, k) *ov2*: controlled natural ventilation for indoor thermal comfort, no HVAC; (c, f, i, l)

326 *ov3*: mixed mode ventilation

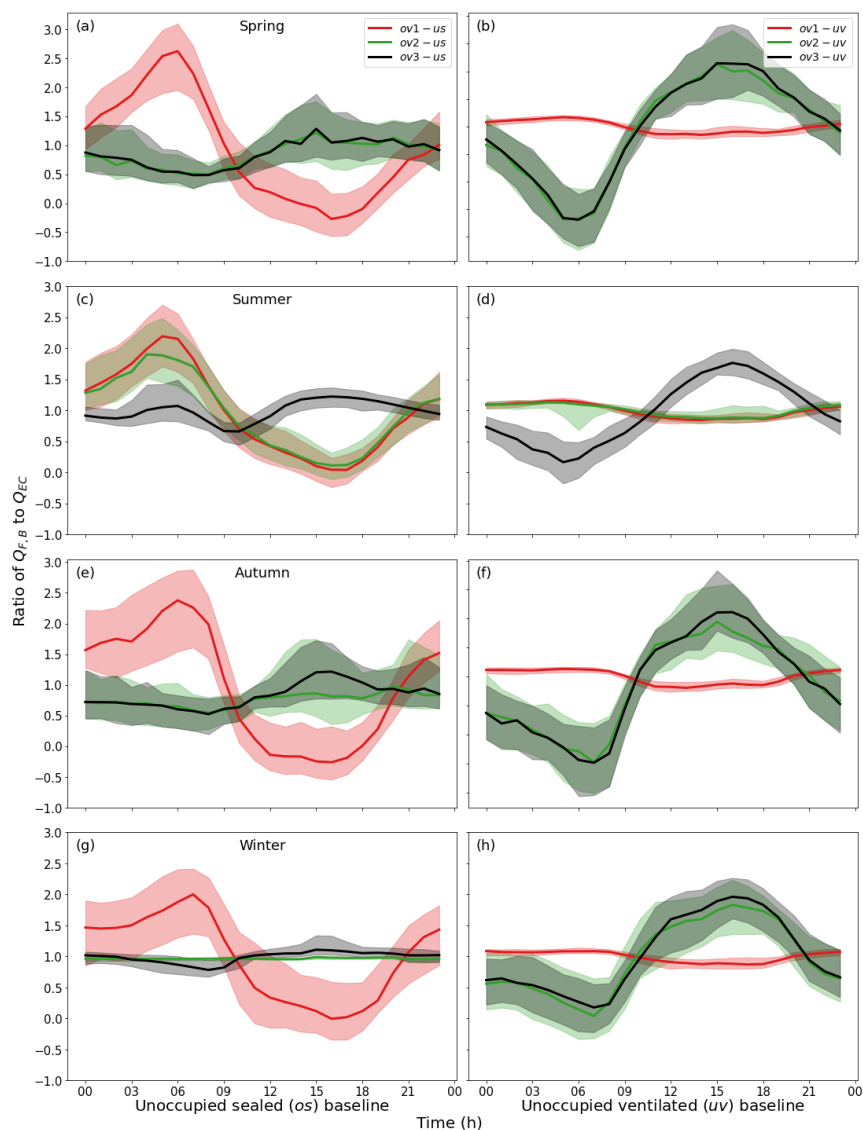


327 **3.3 Impact of unoccupied baseline chosen**

328 Here two unoccupied baselines (*us* - unoccupied sealed building, *uv* - unoccupied ventilated building with
329 uncontrolled open window) are used to assess the impact. A ratio between $Q_{F,B}$ to Q_{EC} (R) is used (Fig. 3) to
330 normalize the impact of baselines on their difference with different building operation modes. The largest
331 difference in R occurs on 23 December at 11:00, with values of 5.13 (*ov3-uv*) and -2.72 (*ov1-us*), reflecting the
332 considerable difference between $Q_{F,B}$ to Q_{EC} .

333 Two diurnal patterns of the R ratio are distinguished. When the window is always open (*ov1* in all seasons,
334 *ov2* in summer), $R > 1$ ($Q_{F,B} > Q_{EC}$) at night/early morning (22:00-08:00), reaching its maximum around
335 05:00-07:00 (near sunrise in all seasons). For the remaining periods, which are relatively warm, $R < 1$. Whereas,
336 when window opening/closing is controlled and HVAC is used for thermal comfort an almost inverse temporal
337 pattern of R occurs, with $R > 1$ during afternoon when either window is open or the air conditioner is activated.
338 The peak R occurs at 15:00 when both outdoor temperature and solar radiation are high.

339 When different unoccupied baselines are used, the temporal patterns of R are similar for all cases, but their
340 magnitudes differ significantly. R is close to 1 when window states between unoccupied and occupied buildings
341 are similar (e.g. *ov1-uv* in all seasons, *ov2-uv* in summer). Hence, greater difference occurs in heat transfer from
342 ventilation or mechanical heating/cooling between occupied and unoccupied building (i.e., larger R). Thus, the
343 baseline chosen impacts the results and require appropriate consideration for incorporating $Q_{F,B}$ into
344 atmospheric modelling.



345
 346 Figure 3: $Q_{F,B}$ to Q_{EC} ratio (R) median (line) and IQR (shading) for (a-b) spring, (c-d) summer, (e-f) autumn and (g-h)
 347 winter, using two unoccupied baselines: (a, c, e, g) sealed (*us*), and (b, d, f, h) ventilation (*uv*); each with three occupancy
 348 types (colour): *ov1*: Only internal heat gains are applied and window is fully open; *ov2*: Internal heat gains and natural
 349 ventilation control are applied. *ov3*: Internal heat gains, natural ventilation control and HVAC system are applied.

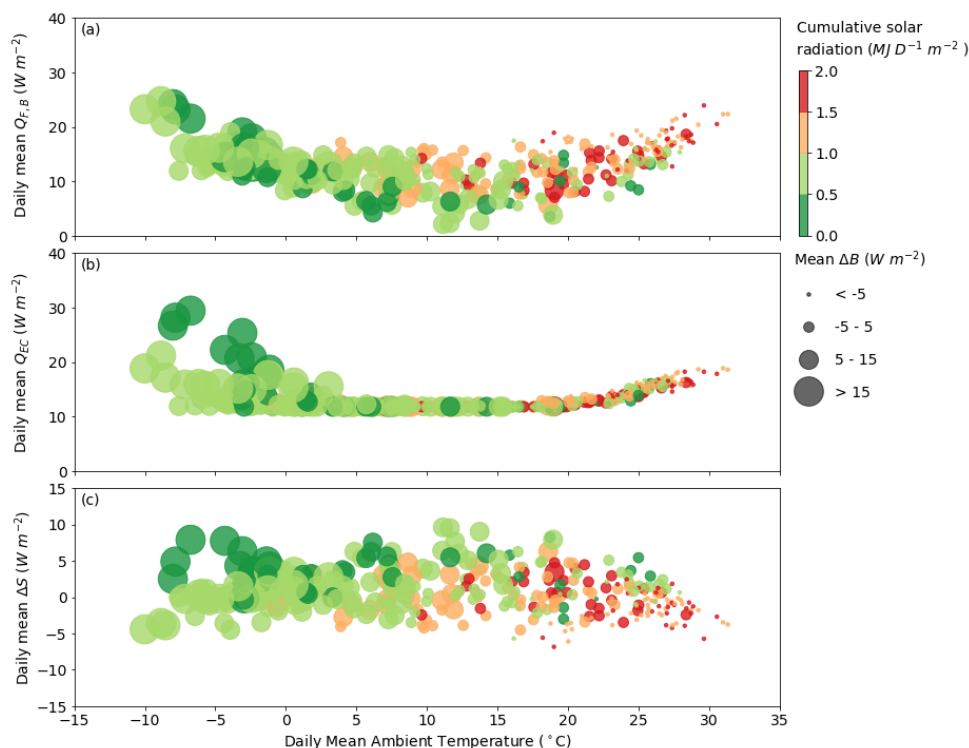
350 3.4 Daily variation of fluxes in relation to meteorological conditions

351 Ambient air temperature is one of the most crucial factors controlling building energy consumption (Sailor and
 352 Vasireddy, 2006). Hence, it is often used to determine daily variability of Q_{EC} (e.g. Lindberg et al., 2013) and
 353 the resulting monthly variations (e.g. Allen et al., 2011). By accounting for ΔS_{0-u_0} in this study, the response of



354 $Q_{F,B}$ to ambient air temperature may differ to previous studies. To examine this we use the *ov3-us* case to
355 consider the relations of daily mean (unless indicated) variables of air temperature (mean), solar radiation (daily
356 total) and simulated available energy to the building from human activities (ΔB) with anthropogenic heat flux
357 ($Q_{F,B}$ in Fig. 4a), energy consumption (Q_{EC} in Fig. 4b) and their difference (ΔS_{o-u_0} in Fig. 4c). The overall
358 trends between $Q_{F,B}$ and Q_{EC} to ambient air temperature are consistent, with $Q_{F,B}$ and Q_{EC} smallest when
359 temperatures are between 10-15°C. This coincides with the Nicol and Humphreys' (2002) monthly balance-point
360 temperature of 12°C, which has been regarded as the equivalent ambient air temperature with the minimum
361 energy use within the building (e.g. Allen et al., 2011, Koralegedara et al., 2016). As the temperature increases
362 (decreases), Q_{EC} increases proportionally with temperature due to mechanical cooling (heating). However, in
363 contrast to Q_{EC} , $Q_{F,B}$ has a much larger variability at the same temperature caused by a large range of ΔS_{o-u_0} (-
364 7.7 to 9.0 W m⁻²), which is highly dependent on human activities on diurnal scale (Sect. 3.1)

365 To understand the large daily variability of ΔS_{o-u_0} , we use ΔB to indicate the effect of human activities
366 (heat addition or removal) in one day. Higher ΔB (larger circles) are associated with higher ΔS_{o-u_0} at the same
367 ambient air temperature, especially in winter (Fig. 4c). This is not unexpected as buildings will absorb more heat
368 when extra internal energy is added into the building. Inversely, negative ΔB (small circles) contributes to much
369 more heat release from heat storage (lower ΔS_{o-u_0} through either natural ventilation or mechanical cooling. The
370 sign and magnitude of ΔB are linked to daily cumulative solar radiation. At the same ambient air temperature,
371 higher solar radiation indicates the need for larger heat removal or less heat addition to the building for thermal
372 comfort, therefore leading to a smaller ΔB and lower ΔS_{o-u_0} . Consequently, we can conclude that both ambient
373 air temperature and cumulative solar radiation are important meteorological factors to determining ΔS_{o-u_0} and
374 $Q_{F,B}$.



375

376 Figure 4: Daily results for the *ov3-us* case stratified by daily cumulative solar radiation (colour) and daily mean available
377 energy to the building (size) (Eq. (9)) associated with human activities, with mean external air (ambient) temperature and (a)
378 mean anthropogenic heat flux, (b) energy consumption and (c) difference in storage heat flux.

379 4 Conclusions

380 Anthropogenic heat flux from buildings ($Q_{F,B}$) is defined as the additional heat released from building into
381 atmosphere due to human activities. It is qualitatively different to building energy consumption (Q_{EC}) in
382 temporal pattern and magnitude as result of thermal inertia of building (Iamarino et al., 2012). However, as there
383 is no standard to quantify ‘real’ $Q_{F,B}$ most studies use Q_{EC} as a proxy via inventory and building energy
384 modelling approaches. This paper proposes a new method to quantify a more appropriate $Q_{F,B}$ by utilising the
385 difference in heat fluxes between an occupied and unoccupied building (i.e. the built structure with absolutely
386 no energy use and human metabolism). We show the difference between Q_{EC} and $Q_{F,B}$ is attributable to a
387 change in the storage heat flux induced by human activities (ΔS_{o-u_0}). $Q_{F,B}$ has four components based on its
388 dissipation pathways, including outgoing longwave radiation, turbulent sensible heat flux (convection), heat
389 release due to air exchange and waste heat from HVAC systems. We use one simplified case study in Beijing to



390 demonstrate the analysis using building energy simulations to quantify the temporal difference between Q_{EC} and
391 $Q_{F,B}$ and understand the relative importance of building operations for thermal comfort and meteorological
392 condition on $Q_{F,B}$. The key conclusions are:

- 393 • Hourly ratios between $Q_{F,B}$ and Q_{EC} can differ between -2.72 and 5.13 because of differences in
394 occupancy use of the building (within a year, in Beijing's climate). Individual ratios frequently exceed
395 3 between 14:00 and 16:00 when controlled natural ventilation or mechanical cooling is activated in
396 shoulder season). Thus, the definitions differences are large.
- 397 • Natural ventilation (ΔBAE_{o-u0}) or HVAC operation ($Q_{Waste,o}$ for cooling and Q_{HVAC} for heating) are
398 two predominant contributors to the storage heat flux. Hence, different building operations to control
399 thermal comfort determine the diurnal profile of $Q_{F,B}$ by affecting not only Q_{EC} but also ΔS_{o-u0} .
- 400 • The day-to-day variation of $Q_{F,B}$ diurnal profile is broader than that of Q_{EC} .
- 401 • Diurnal profile of ΔS_{o-u0} varies with season as occupants modify their behaviours and the interaction
402 with buildings to achieve thermal comfort (e.g. cooling in summer and heating in winter), indicating
403 differences between $Q_{F,B}$ and Q_{EC} will vary with both climate and cultural norms.
- 404 • $Q_{F,B}$ is sensitive to the unoccupied baseline chosen (here two are analysed unoccupied sealed vs
405 unoccupied ventilated). An 'unoccupied baseline' needs to be integrated into urban climate modelling
406 in the future.
- 407 • Daily mean temperature only accounts for the day-to-day variability in Q_{EC} rather than ΔS_{o-u0} . Both
408 ambient air temperature and cumulative solar radiation are important meteorological factors to
409 determine ΔS_{o-u0} and $Q_{F,B}$.

410 Our new approach should be used to provide data for future parameterisations of both anthropogenic heat
411 flux from buildings and storage heat fluxes for urban weather and climate modelling. We conclude that storage
412 heat fluxes in cities could also be modified by occupant behaviour. This theoretical analysis is the first step
413 towards a quantitative understanding on how $Q_{F,B}$ differs from Q_{EC} . Future work should include: (i) Expand
414 beyond our very idealised building archetype and building operation mode, to more complex real-world building
415 types and building operations; (ii) we ignore latent heat release by HVAC system, such as cooling towers, these
416 processes need to be included; and (iii) a wider range of building thermal properties should be explored.

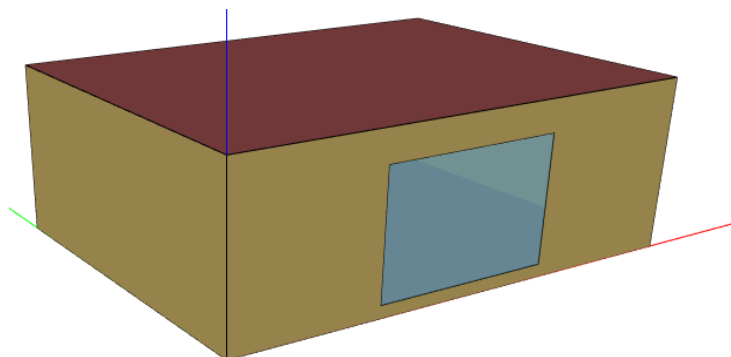
417 **Appendix A: Building energy simulation details**

418 **Table A.1:** Thermal properties of building fabric material (ASHRAE, 2017)



Opaque fabric						
Elements	Thermal conductivity ($\text{W m}^{-1}\text{K}^{-1}$)	Thickness (m)	U-value ($\text{W m}^{-2}\text{K}^{-1}$)	Thermal resistance ($\text{m}^2\text{K}^1\text{W}^{-1}$)	Density (kg m^{-3})	Specific heat ($\text{J kg}^{-1}\text{K}^{-1}$)
<i>Exterior wall (inside to outdoors)</i>						
Interior surface coefficient			8.290	0.121		
Concrete block	0.510	0.100	5.100	0.196	1400	1000
Foam insulation	0.040	0.0615	0.651	1.537	10	1400
Wood siding	0.140	0.009	15.556	0.064	530	900
Exterior surface coefficient			29.300	0.034		
Overall, air to air			0.512	1.952		
<i>Floor (inside to outdoors)</i>						
Interior surface coefficient			8.290	0.121		
Concrete slab	1.130	0.08	14.125	0.071	1400	1000
Insulation	0.040	1.007	0.040	25175	0	0
Overall, air to air			0.039	25.366		
<i>Exterior roof (inside to outdoors)</i>						
Interior surface coefficient			8.290	0.121		
Plasterboard	0.160	0.010	16.000	0.063	950	840
Fiberglass quilt	0.040	0.1118	0.358	2.794	12	840
Roof deck	0.140	0.019	7.368	0.136	536	900
Exterior surface coefficient			29.300	0.034		
Overall, air to air			0.318	3.147		
<i>Transparent fabric (windows)</i>						
Number of panes				2		
Pane thickness (mm)				3.175		
Air-gap thickness (mm)				13		
Normal direct-beam transmittance through one pane				0.86156		
Thermal Conductivity of glass ($\text{W m}^{-1}\text{K}^{-1}$)				1.06		
Exterior combined surface coefficient ($\text{W m}^{-2}\text{K}^{-1}$)				21.00		
Interior combined surface coefficient ($\text{W m}^{-2}\text{K}^{-1}$)				8.29		
U-value from interior air to ambient air ($\text{W m}^{-2}\text{K}^{-1}$)				3.0		
Double-pane solar heat gain coefficient at normal incidence				0.789		

419 **Figure A.1:** Building geometry of ASHRAE 140 case 900 (with changed window)



420

421 **Table A.2:** Composition of internal heat gains from local building code (MOHURD, 2018). Human metabolism rate (100 W
 422 p^{-1}) is typical of resting activities (e.g. sleeping, reclining, seated and standing, 72-126W p^{-1}) (ASHRAE, 2005).

Lighting (W m^{-2})	Equipment (W m^{-2})	Occupancy density (p m^{-2})
5	3.8	0.03

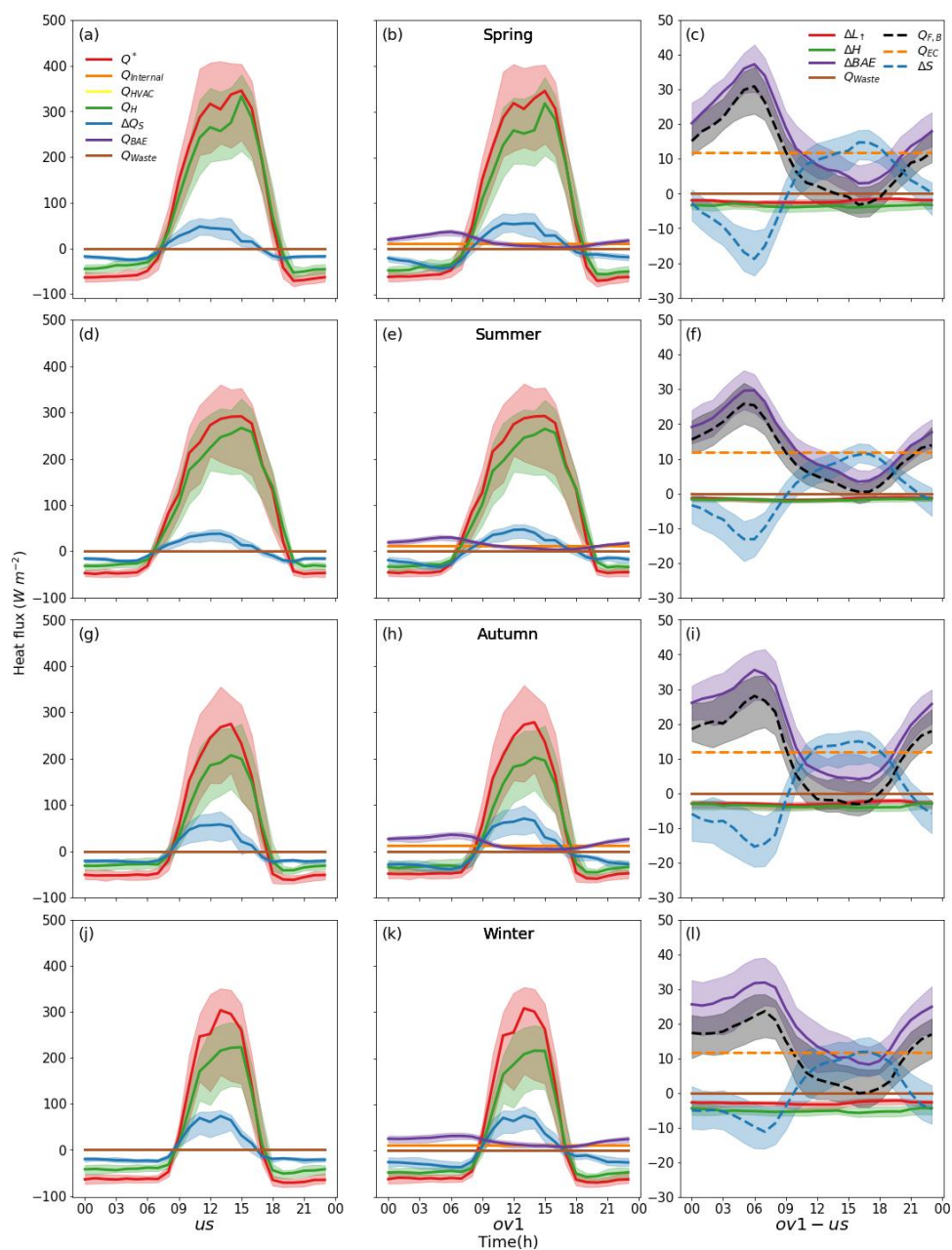


423 **Table A.3:** EnergyPlus output variables are used here in the following equations first. A_{Floor} – is total area of floor of the
 424 building (m^2)

EnergyPlus output variable (Units: W)	Notation	Building volume energy balance fluxes calculated ($W\ m^{-2}$)	Equation (Units: $W\ m^{-2}$)
Outside face net thermal radiation heat gain rate	$l_i - l_r$	Net longwave radiation	$L_r - L_i = \sum_{i=1}^{N_{surface}} (l_r - l_i) / A_{floor}$
Zone total internal total heating rate	$q_{internal}$	Internal heat gains within the whole building	$Q_{internal} = \sum_{i=1}^{N_{zone}} q_{internal} / A_{floor}$
Surface outside face convection heat gain rate	q_H	Turbulent sensible heat flux	$Q_H = - \sum_{i=1}^{N_{surface}} q_H / A_{floor}$
Zone air heat balance air energy storage rate	$\Delta q_{S,a}$	Net storage heat flux for the building volume	$\Delta Q_S = (\sum_{i=1}^{N_{zone}} \Delta q_{S,a} + \sum_{i=1}^{N_{surface}} \Delta q_{S,s}) / A_{floor}$
Surface heat storage rate	$\Delta q_{S,s}$		
AFN (Airflow network) zone exfiltration sensible heat transfer rate	Δq_{BAE}	Heat transfer by air exchange between building and atmosphere	$Q_{BAE} = \sum_{i=1}^{N_{zone}} q_{BAE} / A_{floor}$
Zone ideal loads supply air sensible heating rate	Δq_{HS}	Sensible heating load	$Q_{HS} = \sum_{i=1}^{N_{zone}} q_{HS} / A_{floor}$
Zone ideal loads supply air sensible cooling rate	Δq_{AC}	Sensible cooling load	$Q_{AC} = \sum_{i=1}^{N_{zone}} q_{AC} / A_{floor}$

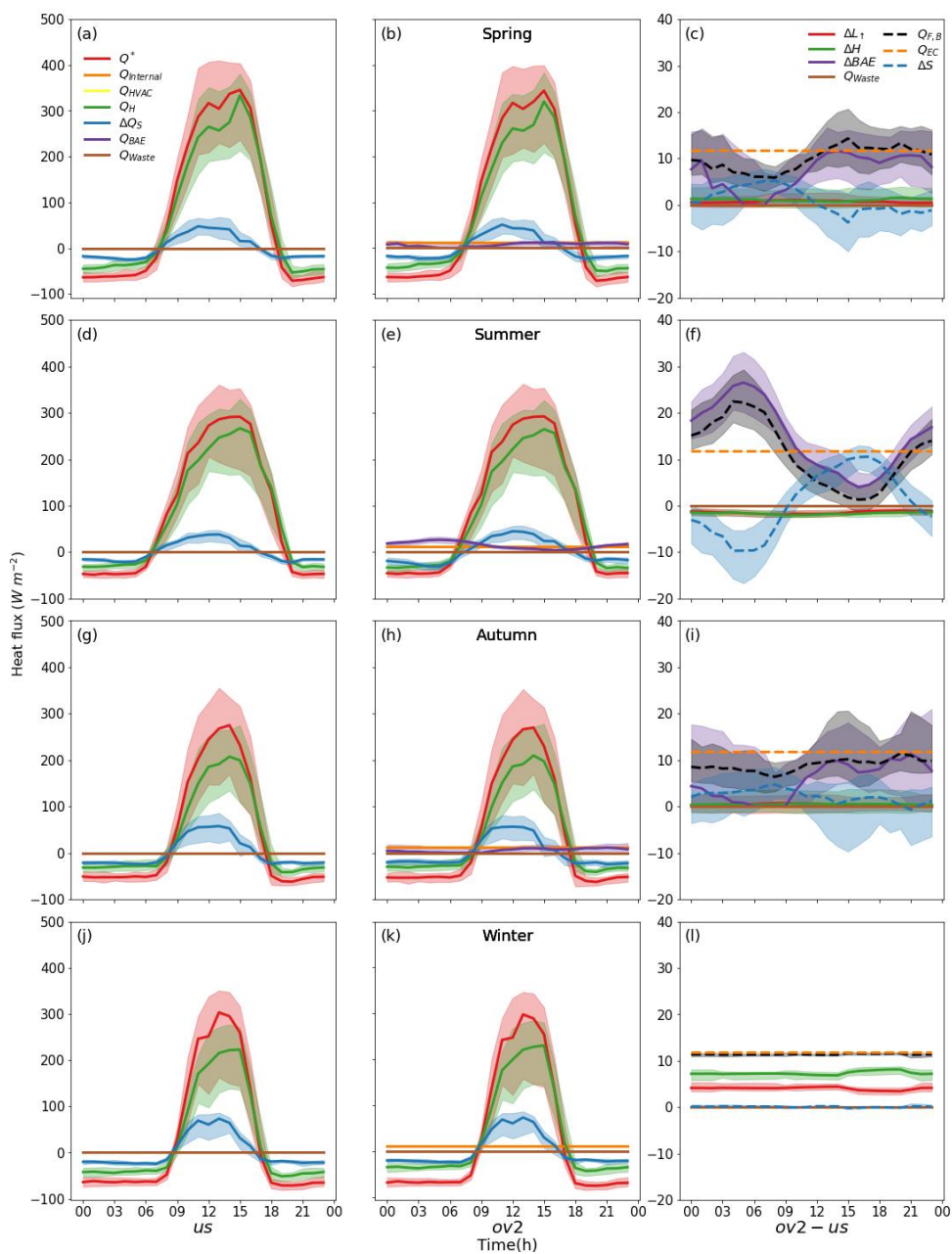


425 **Appendix B: Energy balance analysis for other cases**



426

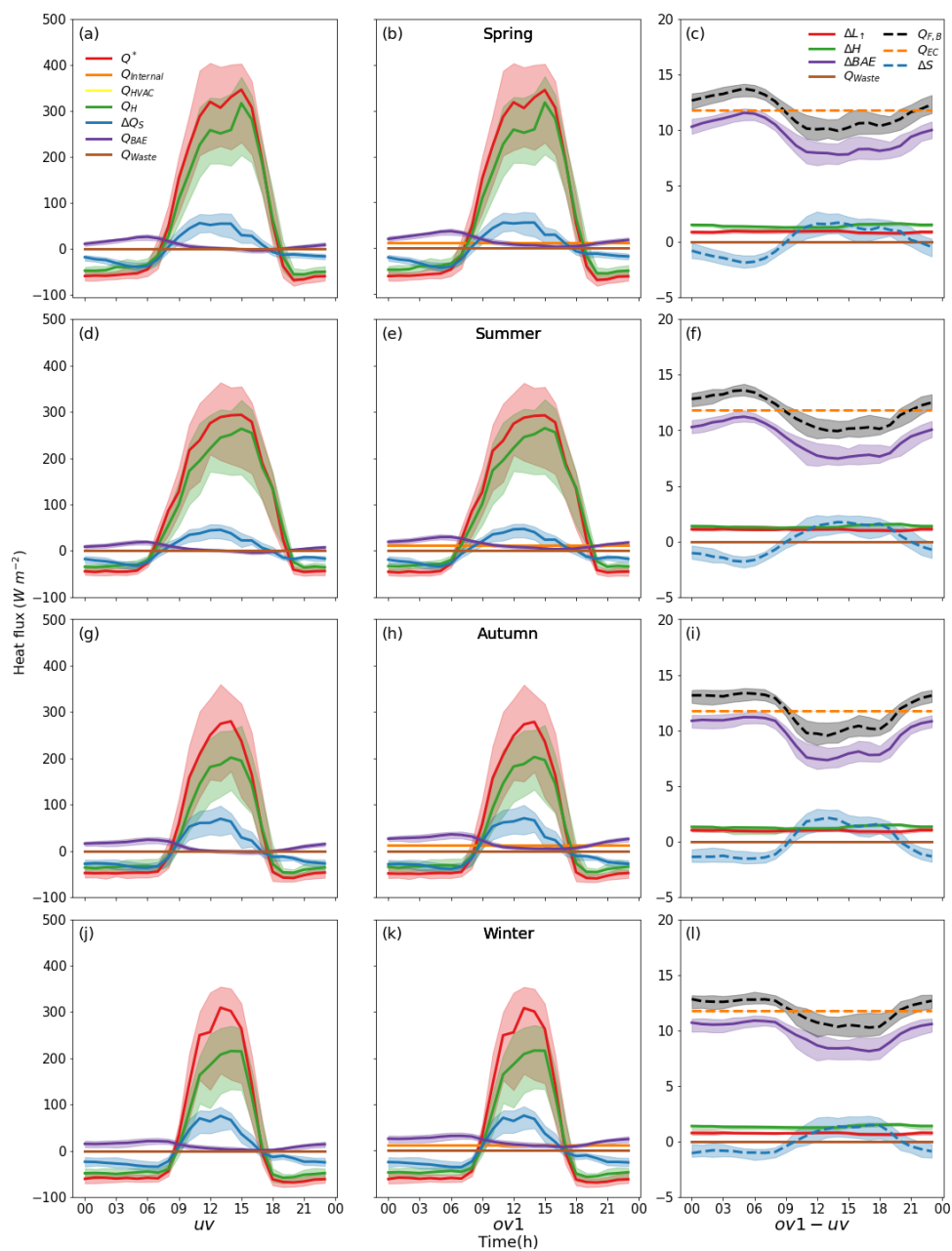
427 Figure B1. As Figure 1, but uses *ov1* for occupied building case in (b, e, h, k) and the heat flux difference with respect to
 428 unoccupied sealed building (*ov1-us*) in (c, f, i, l)



429

430 Figure B2. As Figure B1, but uses *ov2* for occupied building case in (b, e, h, k) and the heat flux difference with respect to

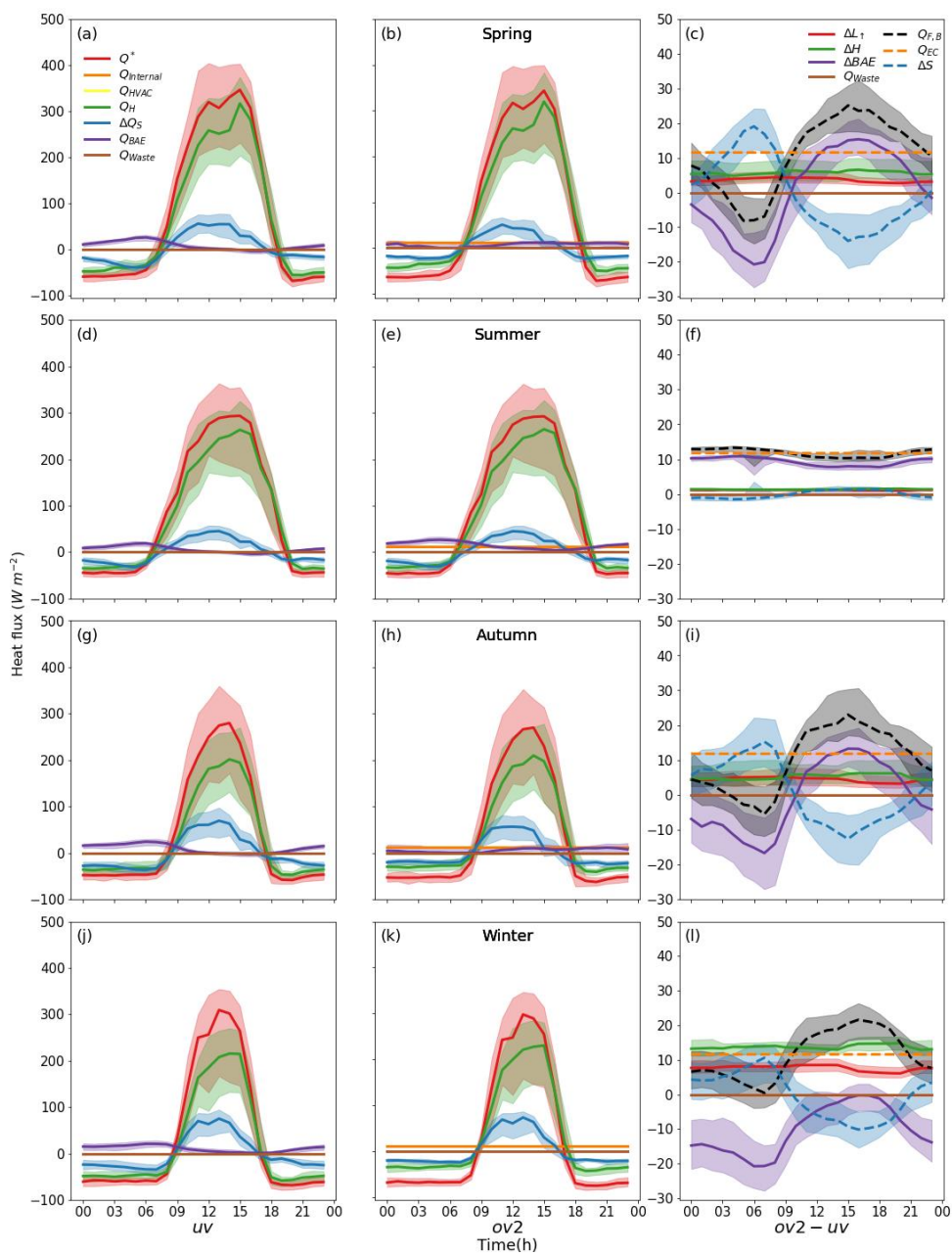
431 unoccupied sealed building (*ov2-us*) in (c, f, i, l)



432

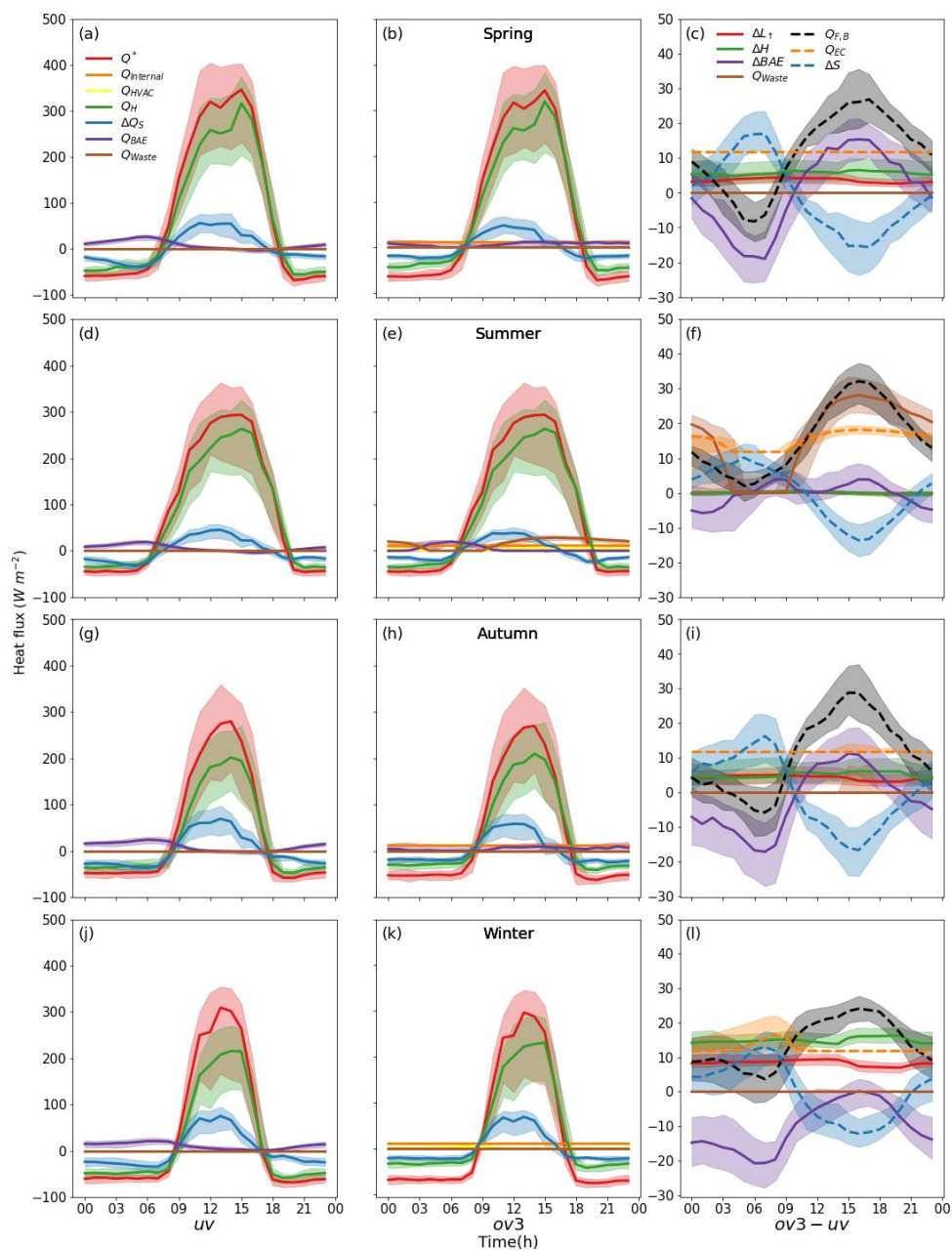
433 Figure B3. As Figure B2, but uses unoccupied ventilation baseline (a, d, g, j) and occupied building case *ov1* in (b, e, h, k)

434 and their difference (*ov1-uv*) in (c, f, i, l)



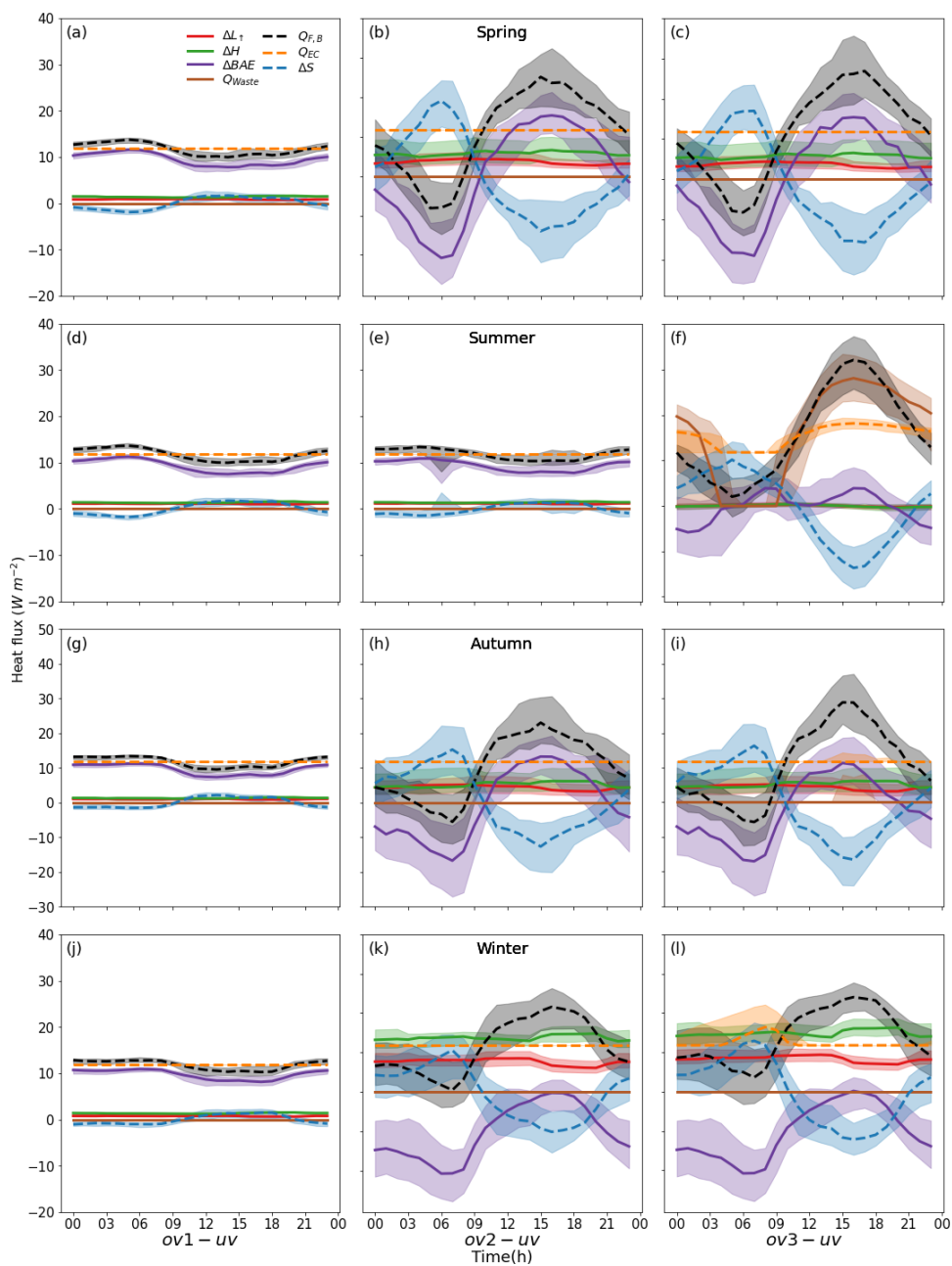
435

436 Figure B4. As Figure B3, but uses occupied building case *ov2* in (b, e, h, k) and their difference (*ov2-uv*) in (c, f, i, l)



437

438 Figure B5. As Figure B3, but with *ov3* in (b, e, h, k) and their difference (*ov3-uv*) in (c, f, i, l)



439

440 Figure B6. As Figure 2 but with uv as the baseline



441 **Acknowledgements**

442 This work is funded as part of NERC-COSMA project (NE/S005889/1), ERC urbisphere (855005) and Newton
443 Fund/Met Office CSSP China Next Generation Cities (SG, ZL)

444 **References**

- 445 Allen, L., Lindberg, F., Grimmond, C.S.B.: Global to city scale urban anthropogenic heat flux: Model and
446 variability, *Int. J. Climatol.*, 31, 1990–2005, <https://doi.org/10.1002/joc.2210>, 2011.
- 447 ASHRAE.: ANSI/ASHRAE Standard 140-2017 Standard method of test for the evaluation of building energy
448 analysis computer programs, American Society of Heating, Refrigerating and Air-Conditioning Engineers,
449 2017.
- 450 Biggart, M., Stocker, J., Doherty, R.M., Wild, O., Carruthers, D., Grimmond, S., Han, Y., Fu, P., Kotthaus, S.:
451 Modelling spatiotemporal variations of the canopy layer urban heat island in Beijing at the neighbourhood scale,
452 *Atmos. Chem. Phys.*, 21, 13687–13711, <https://doi.org/10.5194/acp-21-13687-2021>, 2021.
- 453 Chen, X., Yang, H., Wang, Y.: Parametric study of passive design strategies for high-rise residential buildings
454 in hot and humid climates: miscellaneous impact factors, *Renew. Sustain. Energy Rev.*, 69, 442–460,
455 <https://doi.org/10.1016/j.rser.2016.11.055>, 2017.
- 456 China Meteorological Bureau, Climate Information Center, Climate Data Office and Tsinghua University,
457 Department of Building Science and Technology.: China Standard Weather Data for Analyzing Building
458 Thermal Conditions, Beijing: China Building Industry Publishing House, ISBN 7-112-07273-3 (13228), 2005.
- 459 Chow, W.T.L., Salamanca, F., Georgescu, M., Mahalov, A., Milne, J.M., Ruddell, B.L.: A multi-method and
460 multi-scale approach for estimating city-wide anthropogenic heat fluxes, *Atmos. Environ.*, 99, 64–76,
461 <https://doi.org/10.1016/j.atmosenv.2014.09.053>, 2014.
- 462 Daish, N.C., Carrilho da Graça, G., Linden, P.F., Banks, D.: Impact of aperture separation on wind-driven
463 single-sided natural ventilation, *Build. Environ.*, 108, 122–134, <https://doi.org/10.1016/j.buildenv.2016.08.015>,
464 2016.
- 465 DOE.: EnergyPlus™ Version 9.4.0, <https://energyplus.net/>, 2020.
- 466 DOE.: EnergyPlus™ Version 9.4.0 Input Output Reference, 2020.
- 467 Fan, H., Sailor, D.J.: Modeling the impacts of anthropogenic heating on the urban climate of Philadelphia: A
468 comparison of implementations in two PBL schemes, *Atmos. Environ.*, 39, 73–84,



- 469 <https://doi.org/10.1016/j.atmosenv.2004.09.031>, 2005.
- 470 Fan, S., Davies Wykes, M.S., Lin, W.E., Jones, R.L., Robins, A.G., Linden, P.F.: A full-scale field study for
471 evaluation of simple analytical models of cross ventilation and single-sided ventilation, *Build. Environ.*, 187,
472 107386, <https://doi.org/10.1016/j.buildenv.2020.107386>, 2021.
- 473 Goward, S.N.: Thermal behavior of urban landscapes and the urban heat island, *Phys. Geogr.*, 2, 19–33,
474 <https://doi.org/10.1080/02723646.1981.10642202>, 1981.
- 475 Grimmond, C.S.B.: The suburban energy balance: Methodological considerations and results for a mid-latitude
476 west coast city under winter and spring conditions, *Int. J. Climatol.*, 12, 481–497,
477 <https://doi.org/10.1002/joc.3370120506>, 1992.
- 478 Heiple, S., Sailor, D.J.: Using building energy simulation and geospatial modeling techniques to determine high
479 resolution building sector energy consumption profiles, *Energy Build.*, 40, 1426–1436,
480 <https://doi.org/10.1016/j.enbuild.2008.01.005>, 2008.
- 481 Iamarino, M., Beevers, S., Grimmond, C.S.B.: High-resolution (space, time) anthropogenic heat emissions:
482 London 1970–2025, *Int. J. Climatol.*, 32, 1754–1767, <https://doi.org/10.1002/joc.2390>, 2012.
- 483 Ichinose, T., Shimodozono, K., Hanaki, K.: Impact of anthropogenic heat on urban climate in Tokyo, *Atmos.*
484 *Environ.*, 33, 3897–3909, [https://doi.org/10.1016/S1352-2310\(99\)00132-6](https://doi.org/10.1016/S1352-2310(99)00132-6), 1999.
- 485 Koralegedara, S.B., Lin, C.Y., Sheng, Y.F., Kuo, C.H.: Estimation of anthropogenic heat emissions in urban
486 Taiwan and their spatial patterns, *Environ. Pollut.*, 215, 84–95, <https://doi.org/10.1016/j.envpol.2016.04.055>,
487 2016.
- 488 Lindberg, F., Grimmond, C.S.B., Yogeswaran, N., Kotthaus, S., Allen, L.: Impact of city changes and weather
489 on anthropogenic heat flux in Europe 1995–2015, *Urban Clim.*, 4, 1–15,
490 <https://doi.org/10.1016/j.uclim.2013.03.002>, 2013.
- 491 MOHURD.: Design standard for energy efficiency of residential buildings in severe cold and cold
492 zones, JGJ 26-2018, Ministry of Housing and Urban-Rural Development, People’s Republic of China (in
493 Chinese), 2018.
- 494 Nicol, J.F., Humphreys, M.A.: Adaptive thermal comfort and sustainable thermal standards for buildings,
495 *Energy Build.*, 34, 563–572, [https://doi.org/10.1016/S0378-7788\(02\)00006-3](https://doi.org/10.1016/S0378-7788(02)00006-3), 2002.
- 496 Nie, W.S., Sun, T., Ni, G.H.: Spatiotemporal characteristics of anthropogenic heat in an urban environment: A
497 case study of Tsinghua Campus, *Build. Environ.*, 82, 675–686, <https://doi.org/10.1016/j.buildenv.2014.10.011>,
498 2014.



- 499 Oikonomou, E., Davies, M., Mavrogianni, A., Biddulph, P., Wilkinson, P., Kolokotroni, M.: Modelling the
500 relative importance of the urban heat island and the thermal quality of dwellings for overheating in London,
501 *Build. Environ.*, 57, 223–238, <https://doi.org/10.1016/j.buildenv.2012.04.002>, 2012.
- 502 Oke, T.R., Mills, G., Christen, A., Voogt, J.A.: *Urban Climates*, Cambridge University Press,
503 <https://doi.org/https://doi.org/10.1017/9781139016476>, 2017.
- 504 Sailor, D.J.: A review of methods for estimating anthropogenic heat and moisture emissions in the urban
505 environment, *Int. J. Climatol.*, 31, 189–199, <https://doi.org/10.1002/joc.2106>, 2011.
- 506 Sailor, D.J., Lu, L.: A top-down methodology for developing diurnal and seasonal anthropogenic heating
507 profiles for urban areas, *Atmos. Environ.*, 38, 2737–2748, <https://doi.org/10.1016/j.atmosenv.2004.01.034>,
508 2004.
- 509 Sailor, D.J., Vasireddy, C.: Correcting aggregate energy consumption data to account for variability in local
510 weather, *Environ. Model. Softw.*, 21, 733–738, <https://doi.org/10.1016/j.envsoft.2005.08.001>, 2006.
- 511 Santamouris, M., Papanikolaou, N., Livada, I., Koronakis, I., Georgakis, C., Argiriou, A., Assimakopoulos,
512 D.N.: On the impact of urban climate on the energy consumption of building, *Sol. Energy.*, 70, 201–216,
513 [https://doi.org/10.1016/S0038-092X\(00\)00095-5](https://doi.org/10.1016/S0038-092X(00)00095-5), 2001.
- 514 Sellers, W.D.: *Physical climatology*, University of Chicago Press, 1965.
- 515 Takane, Y., Kikegawa, Y., Hara, M., Grimmond, C.S.B.: Urban warming and future air-conditioning use in an
516 Asian megacity: importance of positive feedback, *npj Clim. Atmos. Sci.*, 2, 1–11,
517 <https://doi.org/10.1038/s41612-019-0096-2>, 2019.
- 518 Wang, H., Chen, Q.: A semi-empirical model for studying the impact of thermal mass and cost-return analysis
519 on mixed-mode ventilation in office buildings, *Energy Build.*, 67, 267–
520 274. <https://doi.org/10.1016/j.enbuild.2013.08.025>, 2013.
- 521 Wang, H., Chen, Q.: A new empirical model for predicting single-sided, wind-driven natural ventilation in
522 buildings, *Energy Build.*, 54, 386–394, <https://doi.org/10.1016/j.enbuild.2012.07.028>, 2012.
- 523 Wang, L., Greenberg, S.: Window operation and impacts on building energy consumption, *Energy Build.*, 92,
524 313–321, <https://doi.org/10.1016/j.enbuild.2015.01.060>, 2015.
- 525 Warren PR.: Ventilation through openings on one wall only, *Heat Transfer in Buildings*, Proceedings of ICHMT
526 seminar. Hemisphere, New York, 1977.
- 527 Yu, Z., Hu, L., Sun, T., Albertson, J., Li, Q.: Impact of heat storage on remote-sensing based quantification of
528 anthropogenic heat in urban environments, *Remote Sens. Environ.*, 262, 112520,

<https://doi.org/10.5194/acp-2021-914>
Preprint. Discussion started: 12 November 2021
© Author(s) 2021. CC BY 4.0 License.



529 <https://doi.org/10.1016/j.rse.2021.112520>, 2021.

530